Non-conventional interaction contributions in permalloy/NiO composite thin films deduced from their static and dynamic magnetization behavior

2008 J. Phys.: Condens. Matter 20 125201

(http://iopscience.iop.org/0953-8984/20/12/125201)

IOP Publishing Journal of Physics: Condensed Matter

J. Phys.: Condens. Matter **20** (2008) 125201 (11pp) doi:10.1088/0953-8984/20/12/125201

Non-conventional interaction contributions in permalloy/NiO composite thin films deduced from their static and dynamic magnetization behavior

F Zighem, Y Roussigné, S-M Chérif and P Moch

Laboratoire des Propriétés Mécaniques et Thermodynamiques des Matériaux, CNRS, Institut Galilée, Université Paris-Nord, Avenue J-B Clément, 93430 Villetaneuse, France

E-mail: zighem@galilee.univ-paris13.fr

Received 11 December 2007, in final form 21 January 2008
Published 25 February 2008
Online at stacks.iop.org/JPhysCM/20/125201

Abstract

A comparative study of thin permalloy films (10.4 nm) interfaced with NiO layers of various thicknesses (6 to 47 nm) is presented. The magnetic parameters deduced from different experimental techniques (Brillouin spectroscopy, ferromagnetic resonance and magnetometric (vibrating sample magnetometry and magneto-optical Kerr effect) investigations) show original characteristics which have not been previously evidenced: (i) for most of the samples studied, the exchange bias field is not parallel or perpendicular to the cooling field, in contrast with the in-plane anisotropy field; (ii) the magnetic properties under an out-of-plane applied magnetic field **H** do not match the calculated ones derived from the usual expression for the density of magnetic energy. We introduce a phenomenological additional term proportional to $\cos[\alpha]$ where α is the angle between **H** and the direction normal to the sample: this non-conventional interaction between NiO and permalloy layers allows us to fit all the experimental data.

(Some figures in this article are in colour only in the electronic version)

1. Introduction

The unusual magnetic properties of thin ferromagnetic (F) films elaborated on an antiferromagnetic (AF) substrate were pointed out nearly 50 years ago [1]. The discovery of the so-called exchange bias field, induced inside the ferromagnetic film by the antiferromagnetic material, has given rise to a large number of publications (see, for example, the review papers of Nogués and Schuller [2] and of Stamps [3]), due to its possible applications which are now abundantly developed [4]. However, the detailed mechanisms of this effect are not completely elucidated in spite of a lot of interesting contributions [5]. On the other hand, the AF/F interface is responsible for additional variations of the ferromagnetic parameters ('classical' anisotropy terms and, in many cases, rotatable anisotropy fields [6–8]) which can exist in other types of interfaces [9], but which render the phenomenological description of the magnetic properties of the studied structures rather complicated. In spite of these difficulties, a reasonably satisfactory fit of the experimentally observed static and dynamic properties can generally be obtained using a conventional model for the magnetic energy density including an appropriate exchange bias field [6–8, 10, 11]. But most of the published studies deal with films subjected to an in-plane applied magnetic field and the validity of the adopted form for this energy density has rarely been tested [6] under an external magnetic field inclined with regard to the plane of the film. We present below a rather exhaustive study of a series of thin (thickness: 10.4 nm) ferromagnetic permalloy films deposited on NiO antiferromagnetic layers of various thicknesses (from 6 up to 47 nm), compared to a control 10.4 nm permalloy film lying on a non-magnetic substrate. It includes quasi-static magnetic determinations (vibrating sample magnetometry: VSM) and dynamic spectroscopic techniques (Brillouin light scattering: BLS and ferromagnetic resonance: FMR). Our results are compared with previous data derived from the magneto-optical Kerr effect (MOKE) [12]. We show that, as long as an in-plane magnetic field is applied parallel to

Table 1. A list of the samples studied.

Sample	C_0	C_6	C_{18}	C_{28}	C_{37}	C_{47}	S_{12}
NiO covering	No	1 side	1 side	1 side	1 side	1 side	2 sides
NiO thickness	0	6 nm	18 nm	28 nm	37 nm	47 nm	2×12 nm

the film, the usual phenomenological approach is able to give an account of the experimental behavior. However, the anisotropy parameters, as well as the direction and the values of the exchange bias field, suffer large variations depending on the NiO thickness and on the elaboration conditions (cooling under magnetic fields of variable strength). In contrast, we experimentally prove that this approach is unable to fit the magnetic properties in the case of an out-of-plane applied magnetic field. The form of the energy density has to be modified in order to fulfill a satisfactory fit in the oblique (or perpendicular) situation: it consists in an additional interfacial interaction term, the contribution of which vanishes in the in-plane geometry. This anisotropy term is an order of magnitude larger than the above mentioned in-plane bias contribution.

Below, we first present the results obtained using the in-plane geometry, after a brief description of the studied samples and of the experimental techniques. We then come to the oblique and perpendicular situations and we propose our phenomenological modified model.

2. Samples studied and experimental techniques

The thin films were prepared by Hurdequint [13] using radio frequency sputtering on a silicon substrate previously covered with a Al_2O_3(10 nm)/Ag(8 nm) bi-layer. The permalloy thickness was fixed (10.4 nm) and the NiO thickness t varied from 0 (control 'bare' permalloy film C_0) to 47 nm. Finally, the composition of the samples is written as Si/Al_2O_3(10 nm)/Ag(8 nm)/NiO(t)/$Ni_{0.80}Fe_{0.20}$(10.4 nm)/Al_2O_3(10 nm). In one other sample the permalloy layer was surrounded by two identical ($t = 12$ nm) NiO films. The studied structures are listed in table 1. The x-ray diagrams show a NiO texture consisting in a mixing of preferential orientations with ⟨111⟩ and ⟨100⟩ directions normal to the films (uncompensated and compensated structures, respectively) [12]. In order to favor the exchange bias, most of the samples were annealed just above the Néel temperature of NiO and subsequently cooled under an in-plane low (0.5 kOe) or high (5 kOe) magnetic field.

The magnetometric measurements were performed by Bouziane using a DMS 1660 vibrating sample magnetometer (VSM) in a magnetic field up to 13.5 kOe applied at different in-plane and out-of-plane angles. In addition, we report MOKE measurements performed on the same samples by Gogol [12]. Ferromagnetic resonance (FMR) and low field absorption measurements in the X-band were performed by Hurdequint [14] using a conventional spectrometer. In addition, we performed microstripe ferromagnetic resonance (MS-FMR) measurements: this method detects a small variation of the HF power transmitted by the strip-line coupled to the sample as a function of the frequency, due to the coupling of the studied film to a high frequency circuit under a fixed applied magnetic field; unfortunately, the signal was found to be very weak in samples containing NiO and, consequently, practically not exploitable. Brillouin backscattering polarized spectra were investigated at room temperature using a previously described instrumental technique involving a 2×3 Fabry–Pérot interferometer [15]. The direction of the illuminating incident light beam (at the wavelength $\lambda = 514.5$ nm) as well as the direction and the amplitude of the applied magnetic field **H** could be varied, thus allowing a rather complete study versus **H** and versus the surface wavevector $\mathbf{Q}_{\parallel}$ of the magnetic excitations. The instrumental resolving power corresponds to about a 400 MHz width at half-maximum and allows one to evaluate the frequencies with an uncertainty of 100 MHz.

3. In-plane applied magnetic field

3.1. Hysteresis VSM measurements

Assuming a uniform static magnetization **M** of the permalloy film, its direction under an in-plane applied magnetic field **H** results from the minimization of the partial energy density E_0, where

$$E_0 = -\mathbf{H}\cdot\mathbf{M} - \frac{k}{M^2}(\mathbf{M}\cdot\mathbf{u})^2 - \frac{j}{M}(\mathbf{M}\cdot\mathbf{v}). \qquad (1)$$

u and **v** are unit vectors lying in the plane of the film; $(j/M)\mathbf{v}$ represents the exchange bias field $\mathbf{H}_b$ and has to vanish in the control sample (absence of NiO); $(2k/M)\mathbf{u}$ represents an in-plane anisotropy field $\mathbf{H}_{a\parallel}$ and is expected to be very small in the control sample. It is often assumed that both **u** and **v** are aligned along the antiferromagnetic sublattice magnetization and that, in a number of cases, this sublattice magnetization is parallel to the cooling field $\mathbf{H}_{\mathbf{cool}}$ [16]: in such cases, for **H** parallel to the cooling field an open hysteresis cycle is observed and allows us to determine H_b (shift from the origin) and $H_{a\parallel}$ (half-width of the cycle); in contrast, for **H** perpendicular to the cooling field, an unshifted reversible variation when sweeping the applied field is expected. Typical observed hysteresis cycles of the samples prepared under a high field cooling are reported in figure 1 for both orientations (i.e., $\mathbf{H} \parallel \mathbf{H}_{cool}$ and $\mathbf{H} \perp \mathbf{H}_{cool}$). As expected, measurable bias or anisotropy fields are not present in the control film. For the thinnest NiO thickness (6 nm: sample C_6), substantial in-plane anisotropy is observed but bias is absent. The remaining samples show both bias and anisotropy. However, at first glance, except for the symmetrically NiO surrounded film (S_{12}), the magnetic properties of those samples are not consistent with **u** and **v** parallel to $\mathbf{H}_{cool}$ but are reminiscent of the expected ones for **u** and **v** perpendicular to $\mathbf{H}_{cool}$: for **H** perpendicular to $\mathbf{H}_{cool}$,

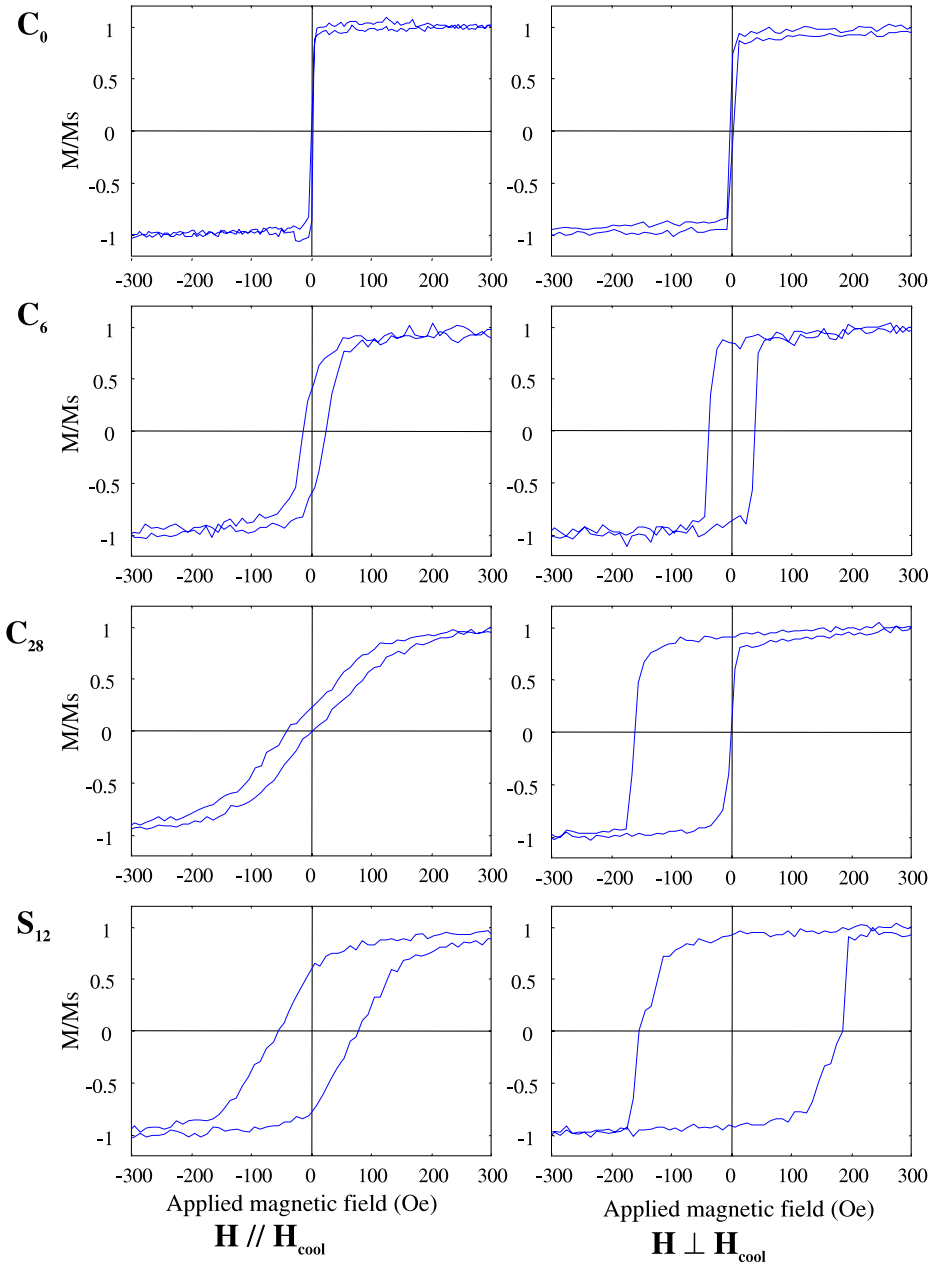

Figure 1. Hysteresis cycles of samples prepared under a high field cooling (5 kOe). The normalized magnetization is plotted versus the applied magnetic field.

they show a widely open hysteresis cycle significantly shifted from the origin. This result is presumably due to the large value of the applied cooling field which favors the spin-flop of the antiferromagnetic NiO film, thus inducing a bias field parallel to the antiferromagnetic sublattice direction, as usually stated [16]. However, it results from a careful examination that such a simple model is not completely satisfactory: the observed cycle measured along the hard axis direction suffers a small shift from the origin; moreover, it is slightly open. These results suggest introducing anisotropy and exchange bias components along this hard direction: we conclude that **u** and **v** are not parallel or perpendicular to the cooling field. It then becomes possible to simulate the observed cycles using equation (1). Such a phenomenological model was previously used in slightly different contexts [17]. In figure 2 we show an approximate fit to the experimental data assuming that **u** is perpendicular to the cooling field but that **v** is inclined versus **u**: it provides the measured shifts from the origin for both parallel and perpendicular geometry; however, this approximation does not lead to an opening of the cycle for $\mathbf{H} \perp \mathbf{u}$, and thus, is not completely satisfying. It is possible to induce simultaneous shift and opening in both cycles through an additional rotation of **u**. However, the experimental results only slightly depart from the calculated ones and the search of a perfect fit is probably artificial. On the other hand, it clearly results from the Brillouin measurements described in the following section that the bias field is not parallel to the anisotropy field. We have then chosen to fit the experimental

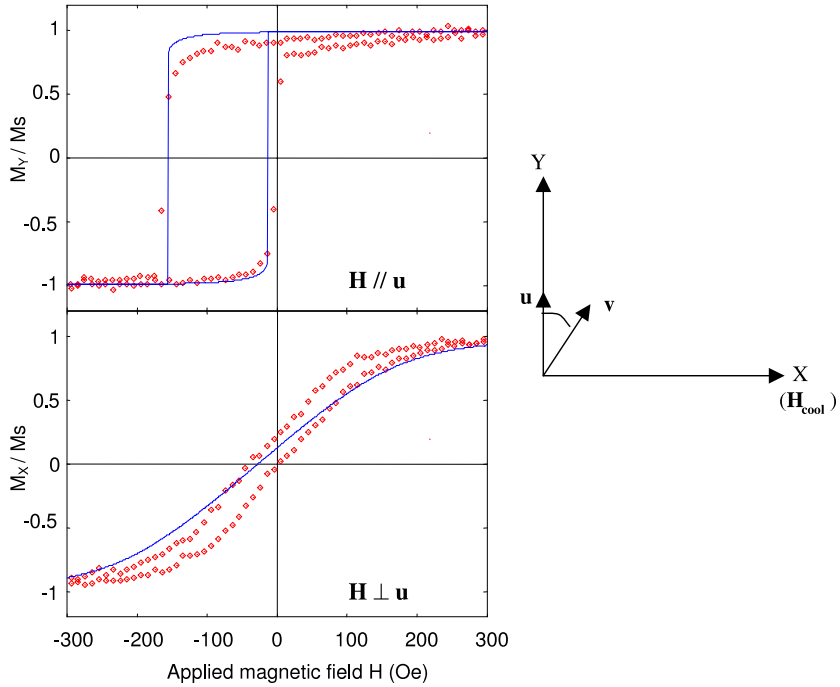

Figure 2. Typical approximate fit to the experimental results for sample C_{28}. Fitting parameters (full lines): $H_{a\parallel} = 140$ Oe; $H_b = 90$ Oe; $(\hat{\mathbf{u}}, \mathbf{v}) = 20°$.

Table 2. Compared values of in-plane anisotropy ($\mathbf{H}_{a\parallel}$), exchange bias ($\mathbf{H}_b$) and rotatable anisotropy ($\mathbf{H}_{rot}$) fields in the studied samples (not measured: n.m.). Only BLS measurements allow us to evaluate the rotatable anisotropy. In this table, the analysis of the FMR [14] and MOKE data [12] assumes that **u** and **v** are parallel to each other. Concerning the line labeled FMR, the values between parentheses are derived from low field absorption measurements.

	Sample	C_0	C_6	C_{18}	C_{28}	C_{37}	C_{47}	S_{12}
BLS	$H_{a\parallel}$ (Oe)	0	30	30	50	50	n.m.	n.m.
	H_b (Oe)	0	0	11	48	48	n.m.	n.m.
	$(\hat{\mathbf{u}}, \mathbf{v})$ (deg)	—	—	27	18	18	n.m.	n.m.
	H_{rot} (Oe)	0	−30	−190	−120	−120	n.m.	n.m.
VSM	$H_{a\parallel}$ (Oe)	0	40	140	140	130	120	170
	H_b (Oe)	0	0	60	90	90	70	9
	$(\hat{\mathbf{u}}, \mathbf{v})$ (deg)	—	—	25	20	20	20	32
MOKE	$H_{a\parallel}$ (Oe)	2	37	62.5	73	n.m.	n.m.	n.m.
	H_b (Oe)	0	0	35	79.5	n.m.	n.m.	n.m.
FMR	$H_{a\parallel}$ (Oe)	(1)	(33)	(61)	(84)	n.m.	(63)	(96)
	H_b (Oe)	(0)	0 (0)	29 (47)	51 (71)	n.m.	45 (65)	29 (50)

magnetometric measurements using a protocol in which **u** is fixed while the amplitudes of the anisotropy field and of the exchange bias field as well as the inclination of **v** over **u** are varied. The results are given in table 2. They are compared to the independently obtained estimations using the FMR [14] and MOKE techniques [12], when available. Notice that, the FMR and MOKE results were analyzed assuming $\mathbf{u} = \mathbf{v}$, which can explain discrepancies which appear in table 2. For the symmetrically NiO surrounded sample, the anisotropy field looks parallel to the cooling field, in contrast with the other films which show an anisotropy field perpendicular to the cooling field. It appears that both anisotropy and exchange bias fields vary from sample to sample but that they show the same order of magnitude. A convincing interpretation is still lacking.

3.2. Magnetic Brillouin scattering

While the static equilibrium under an in-plane applied magnetic field only depends upon E_0 (given by equation (1)), the conventional appropriate density of energy is written as

$$E = E_0 - \frac{K}{M^2}(\mathbf{M} \cdot \mathbf{z})^2 + E_{ex.} + E_{dip.} \qquad (2)$$

where **z** is a unit vector normal to the film: the first additional term is connected to the perpendicular anisotropy field

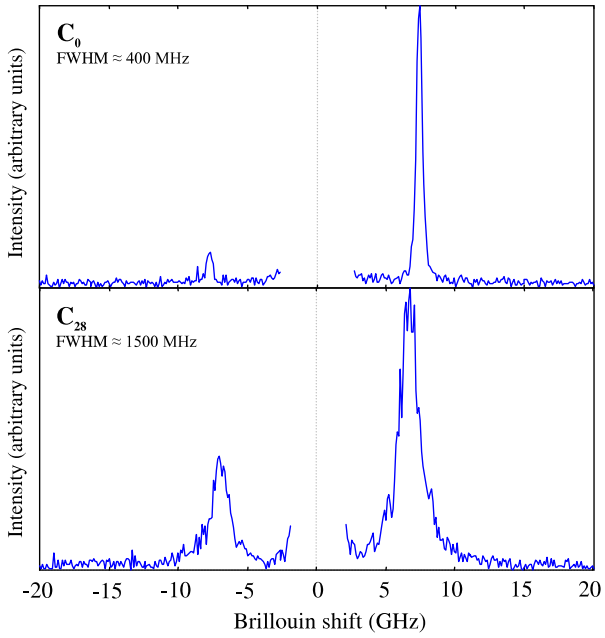

Figure 3. Compared spectra of the C_0 and C_{28} samples. Notice that for the control sample C_0 the lines are sharper and show a larger Stokes/anti-Stokes asymmetry.

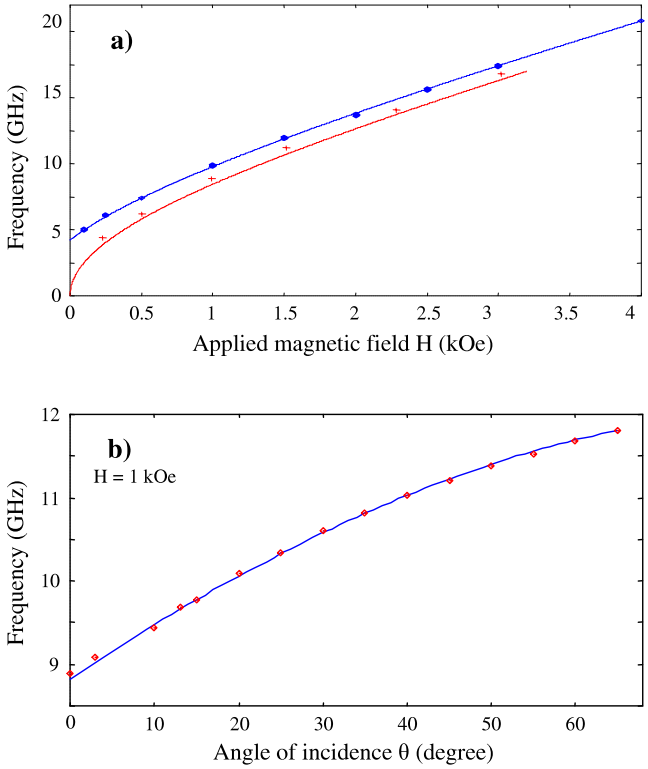

Figure 4. Best fits for the observed Brillouin frequency variations in the control sample: (a) versus the magnetic field with $\mathbf{H} \parallel \mathbf{Q}_\parallel$ (crosses: $Q_\parallel = 2.02 \times 10^5$ cm^{-1}) and $\mathbf{H} \perp \mathbf{Q}_\parallel$ (points: $Q_\parallel = 6.32 \times 10^4$ cm^{-1}); (b) versus the angle of incidence θ (Brillouin scattering with $\mathbf{H} \perp \mathbf{Q}_\parallel$) for $H = 1$ kOe. Calculated variations with $4\pi M_{\rm eff} = 8000$ G, $\gamma = 1.846 \times 10^7$ Hz G^{-1}, $A = 1 \times 10^{-6}$erg cm^{-1}.

$\mathbf{H}_{a\perp} = \frac{2K}{M}\mathbf{z}$ and the second one gives rise to an exchange field which is generally written as $\frac{2A}{M^2}\Delta\mathbf{M}$, where A is the exchange stiffness constant. The last term stands for the dipolar energy. In a film of thickness d, assuming that $Q_\parallel d \ll 1$ [18, 19], the frequency of a propagating magnetic excitation is given by

$$\frac{\omega^2}{\gamma^2} = H_1 H_2 \tag{3}$$

with

$$H_1 = H_{\rm eff} - \frac{2K}{M} + \frac{4\pi M}{1 + dQ_\parallel/2} + \frac{2AQ_\parallel^2}{M}$$

$$H_2 = H_{\rm eff} - \frac{2k}{M^3}\|\mathbf{u}\wedge\mathbf{M}\|^2 + \frac{4\pi}{dQ_\parallel(2+dQ_\parallel)}\frac{\|\mathbf{M}\wedge d\mathbf{Q}_\parallel\|^2}{M} + \frac{2AQ_\parallel^2}{M}$$

and

$$H_{\rm eff} = \frac{\mathbf{H}\cdot\mathbf{M}}{M} + \frac{2k}{M^3}(\mathbf{u}\cdot\mathbf{M})^2 + \frac{j}{M^2}\mathbf{v}\cdot\mathbf{M}.$$

However, it has been found [6] that a better account of the experimental results is generally obtained by introducing an additional rotatable anisotropy field which shifts the frequency. In equation (3), $\mathbf{H}$ has to be replaced by $(\mathbf{H} + \mathbf{H}_{\rm rot})$: the dynamic properties are relevant for an additional field of fixed amplitude, the rotatable anisotropy field $\mathbf{H}_{\rm rot}$, which aligns along the applied field $\mathbf{H}$. Our Brillouin scattering measurements for an in-plane applied field were analyzed using this model. In order to discuss the results it is convenient to make a distinction between the studies performed under a high magnetic field ($H \gtrsim 500$ Oe) and the studies under a low magnetic field ($H \lesssim 500$ Oe).

3.2.1. High magnetic field spectra. In view of the small values of H_b, of $H_{a\parallel}$ and, presumably, of $H_{\rm rot}$, these parameters can be neglected for analyzing the high field spectra. Moreover, it is easy to show that, due to the limited experimental precision, $4\pi M$ and $H_{a\perp}$ cannot be evaluated separately: practically, the frequencies of the observed lines only depend on $4\pi M_{\rm eff} = (4\pi M - H_{a\perp})$ and, to a lesser extent, on A. Consequently, there is only access to $4\pi M_{\rm eff}$. In figure 3, we show two typical spectra, related to the control sample and to a film lying on NiO, respectively. In the first case the observed linewidth of the magnetic Brillouin line does not exceed the instrumental limit. In contrast, a significant broadening can be measured for films deposited on NiO: the full width at half-maximum exceeds 1 GHz, as previously observed [20]. Also notice that the well-known Stokes/anti-Stokes asymmetry of the scattered intensity is reduced in samples containing NiO. In figure 4, we show the observed frequency variations versus H, for $\mathbf{H}$ parallel to $\mathbf{Q}_\parallel$ as well as for $\mathbf{H}$ perpendicular to $\mathbf{Q}_\parallel$, and for $\mathbf{H}$ perpendicular to $\mathbf{Q}_\parallel$ versus the angle of incidence θ (which is related to the wavevector amplitude $Q_\parallel$ through the relation $Q_\parallel = 4\pi\sin[\theta]/\lambda$). They are compared to the calculated ones using our best fitted values of $4\pi M_{\rm eff}$ and of A: it can be seen that the agreement between calculated variations and experimentally observed values is very good.

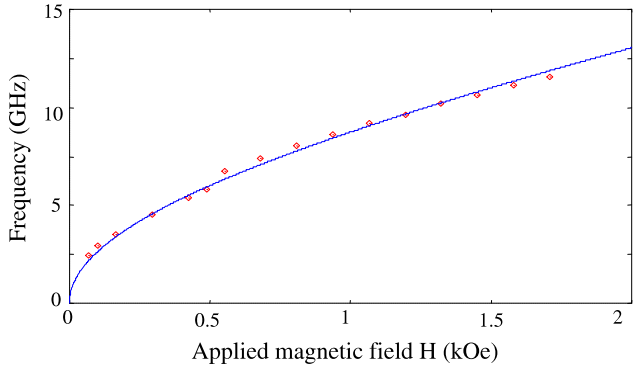

Figure 5. Best fit for the observed FMR (strip-line measurements) frequency variation versus the magnetic field in the control sample. Used parameters: $4\pi M_{\text{eff}} = 7900$ G, $\gamma = 1.846 \times 10^7$ Hz G^{-1}.

Table 3. Values of $4\pi M_{\text{eff}}$ and of the perpendicular anisotropy field $H_{a\perp}$ calculated from the Brillouin data for an in-plane applied magnetic field. M_{eff} is the effective magnetization. $H_{a\perp}$ is obtained assuming that $4\pi M$ (where M stands for the magnetization) is equal to the bulk value, 10 000 G.

Sample	C_0	C_6	C_{18}	C_{28}	C_{37}	C_{47}	S_{12}
(5 kOe cooled)							
$4\pi M_{\text{eff}}$ (kG)	8	4.6	6.4	6.95	6.7	5.2	6.25
$H_{a\perp}$ (kOe)	2	5.4	3.6	3.05	3.3	4.8	3.75
(0.5 kOe cooled)							
$4\pi M_{\text{eff}}$ (kG)	8	4.1	n.m	6.2	5.9	n.m	4.8
$H_{a\perp}$ (kOe)	2	5.9	n.m	3.8	4.1	n.m	5.2

The precision upon the determination of A is rather poor since the frequencies only weakly depend on this parameter. A value of 10^{-6} erg cm^{-1} provides a satisfactory fit for all the samples. In table 3 we present the obtained determinations of $4\pi M_{\text{eff}}$ deduced from the observed frequency variations for all the studied samples. In principle, it would be possible to derive M from the magnetometric measurements by VSM. However, the precision is poor and, consequently, for the evaluation of $H_{a\perp}$, we preferred to assume that, in our samples, M keeps the value usually estimated for bulk permalloy ($4\pi M = 10$ kG). The deduced determinations of $H_{a\perp}$ are listed in table 3: $H_{a\perp}$ significantly varies from sample to sample as often observed [7] and always exceeds 2 kOe. The anisotropy fields are larger in the films cooled in a 0.5 kOe field than in the films cooled in a 5 kOe field. A disordered arrangement of the antiferromagnetic domains probably originates a large anisotropy field; the application of a large cooling field decreases this disorder and, consequently, decreases the anisotropy field. FMR measurements performed by Hurdequint [14] essentially provide the same results, which are also confirmed, at least for the control sample C_0, as shown in figure 5, by our own observations using the strip-line technique (MS-FMR).

3.2.2. Low magnetic field spectra. When the magnitude of the applied field is of the order of $H_{a\parallel}$, H_b and H_{rot}, the anisotropy associated with these parameters induces large frequency variations versus the direction of propagation of the

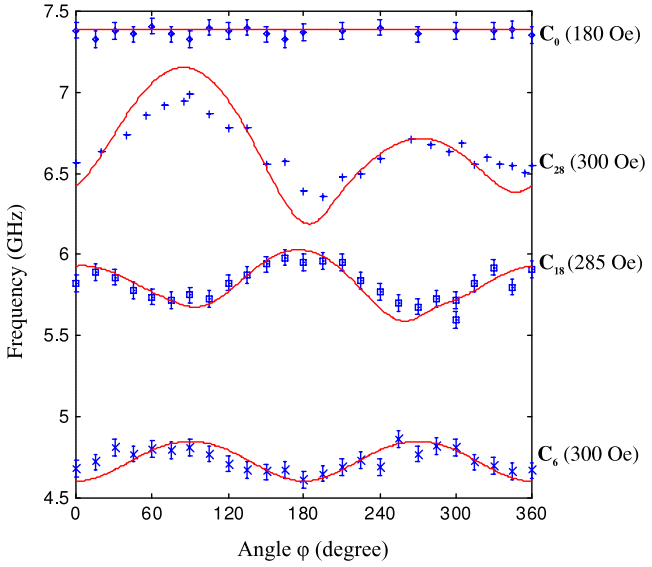

Figure 6. Brillouin frequency variations versus the angle between $\mathbf{Q}_\parallel$ and the direction of $\mathbf{H}_{\text{cool}}$ for low in-plane applied magnetic field. The values of the applied fields are 180, 300, 285 and 300 Oe for samples C_0, C_6, C_{18} and C_{28}, respectively. The full lines represent the best fits, obtained using the parameters given in tables 2 and 3.

studied spin waves, thus allowing the experimental evaluation of those parameters [7, 11, 20, 21]. In figure 6, we present, for different samples, the variations of the frequency versus the angle φ between $\mathbf{Q}_\parallel$ and the direction of the cooling field. The data were obtained with the help of rotation of the films around their normal axis. The analysis uses the values of M_{eff} (and of A) derived from the study under the high magnetic field described in the previous subsection. As expected, in the control sample, the measured frequency does not depend on φ. For the films which show a measurable bias, in most cases a satisfactory fit cannot be obtained with $\mathbf{H}_b$ parallel or perpendicular to the cooling field, thus confirming the oblique character of the bias field, suspected from the magnetometric observations. In table 2, we list the values of $\mathbf{H}_{a\parallel}$, $\mathbf{H}_b$ and $\mathbf{H}_{\text{rot}}$ providing the best fits to our Brillouin spectra. The Brillouin determinations of $H_{a\parallel}$ and H_b are significantly smaller than the ones obtained by VSM: analogous differences between low and high frequency results have been reported [10, 21]. Finally, MOKE [12] and FMR [14] results are also given for comparison. An attempt to interpret the dependence of the measured magnetic parameters on the experimental techniques used was proposed by Fermin *et al* [21]: they introduce an additional term in the energy density related to the formation of a domain wall in the antiferromagnetic NiO sublayer; this term induces a torque which acts on the magnetic dynamics. However, this hypothesis does not provide a complete quantitative coherent description of the observed magnetic properties. In the case of the samples that we studied we did not obtain a significant improvement by considering a domain wall energy term and, consequently, we ignored it. In contrast, the non-collinearity of $\mathbf{H}_{a\parallel}$ and $\mathbf{H}_b$, which, to our knowledge, has never been considered, plays a crucial role in the analysis of our experimental results. Finally, we observe that the rotatable field appropriate to fit our spectra is opposite

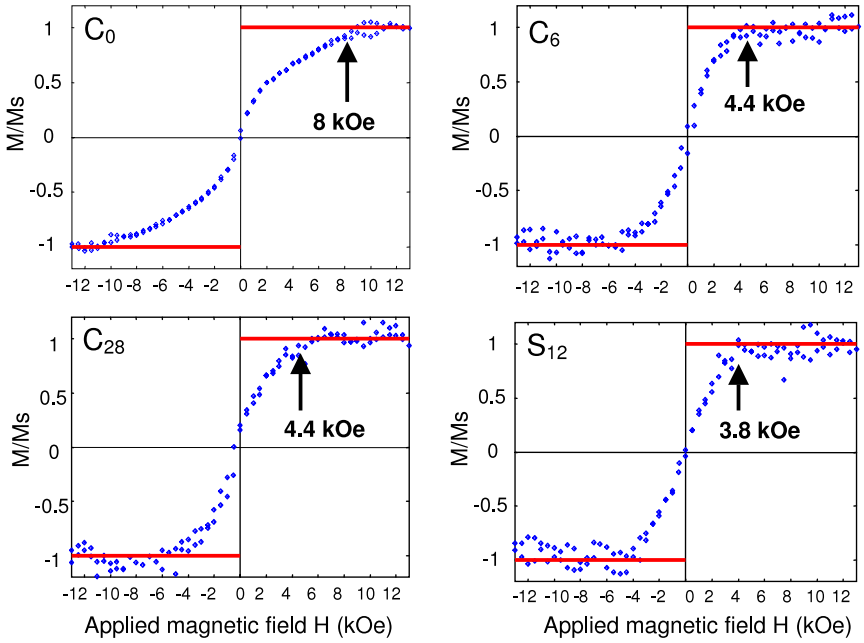

Figure 7. Typical magnetization (VSM) measurements versus a magnetic field applied perpendicularly to the films: the deduced approximate value of $4\pi M_{\text{eff}}$ is shown on each graph.

to **H** (which justifies the negative values reported in table 2): this behavior differs from the usually obtained ones [6, 7]. However, we have observed negative rotatable fields in other systems [22].

4. Out-of-plane applied magnetic field

The calculation of the equilibrium positions and of the spin wave frequencies using expression (2) for the density of energy is straightforward for any direction of the field. However, in this section we focus our attention on experimental situations for which the applied field is large compared to $H_{a\|}, H_b$ and H_{rot} and, then, we shall neglect the contribution of these three parameters.

4.1. VSM measurements under a perpendicular applied field

Within the above approximation, one expects a linear variation from $-M$ to $+M$ of the component of the magnetization along **H** when the applied field varies from $-(4\pi M - H_{a\perp})$ to $+(4\pi M - H_{a\perp})$. Experimentally, the variation of the magnetization versus the applied field is not truly linear, and the determination of the saturation field is not straightforward. In figure 7, we show the most plausible determination of this saturation field. This saturation field differs from the above evaluations $(4\pi M - H_{a\perp})$, with the values of $H_{a\perp}$ derived in the preceding section from the analysis of the Brillouin spectra using an in-plane applied magnetic field. For this geometrical arrangement, in films deposited on NiO, the perpendicular anisotropy field seems increased by $\Delta H_{a\perp}$. The measured values of $\Delta H_{a\perp}$, which have the same order of magnitude as $H_{a\perp}$, i.e. a few kOe, are listed in table 4.

Table 4. Additional anisotropy parameter for the magnetic energy density. The appropriate energy density is obtained by subtracting $(\Delta H_{a\perp}/2M)\cos[\alpha]$ from expression (2), where α is the angle between the applied field and the direction normal to the films.

Sample	C_0	C_6	C_{18}	C_{28}	C_{37}	C_{47}	S_{12}
$\Delta H_{a\perp}$-BLS (kOe)	0	1.3	2.25	2.35	1.9	1.7	2.75
$\Delta H_{a\perp}$-VSM (kOe)	0	2.8	1.6	2.55	1.7	1.35	2.45

4.2. Magnetic Brillouin scattering

4.2.1. Perpendicular applied field. At zero wavevector, when neglecting the $H_{a\|}$, H_b and H_{rot} contributions, the simplified form of expression (2) leads to

$$\omega = 0 \qquad \text{for } H < 4\pi M_{\text{eff}} \tag{4a}$$

$$\omega = \gamma(H - 4\pi M_{\text{eff}}) \qquad \text{for } H > 4\pi M_{\text{eff}}. \tag{4b}$$

For $Q_\| \neq 0$, an indeterminacy appears, due to the absence of a preferential direction of **M**, since the frequency depends on the angle ψ between $\mathbf{Q}_\|$ and $\mathbf{M} \wedge \mathbf{z}$. However, for $H > 4\pi M_{\text{eff}}$ the frequency is not significantly modified:

$$\omega \sim \gamma(H - 4\pi M_{\text{eff}}) \qquad \text{for } H > 4\pi M_{\text{eff}}. \tag{5a}$$

In contrast, for $H < 4\pi M_{\text{eff}}$,

$$\frac{\omega}{\gamma} \approx \cos[\psi]\left(\frac{\mathrm{d}Q_\|}{2}\right)^{0.5}\left\{4\pi M(4\pi M - H_{a\perp}) \times \left(1 - \left(\frac{H}{4\pi M_{\text{eff}}}\right)^2\right)\right\}^{0.5} \qquad \text{for } H < 4\pi M_{\text{eff}} \tag{5b}$$

The above expressions neglect the exchange contribution which only slightly affects the frequencies. The case $H < 4\pi M_{\text{eff}}$, which allows the frequency to sweep a large interval

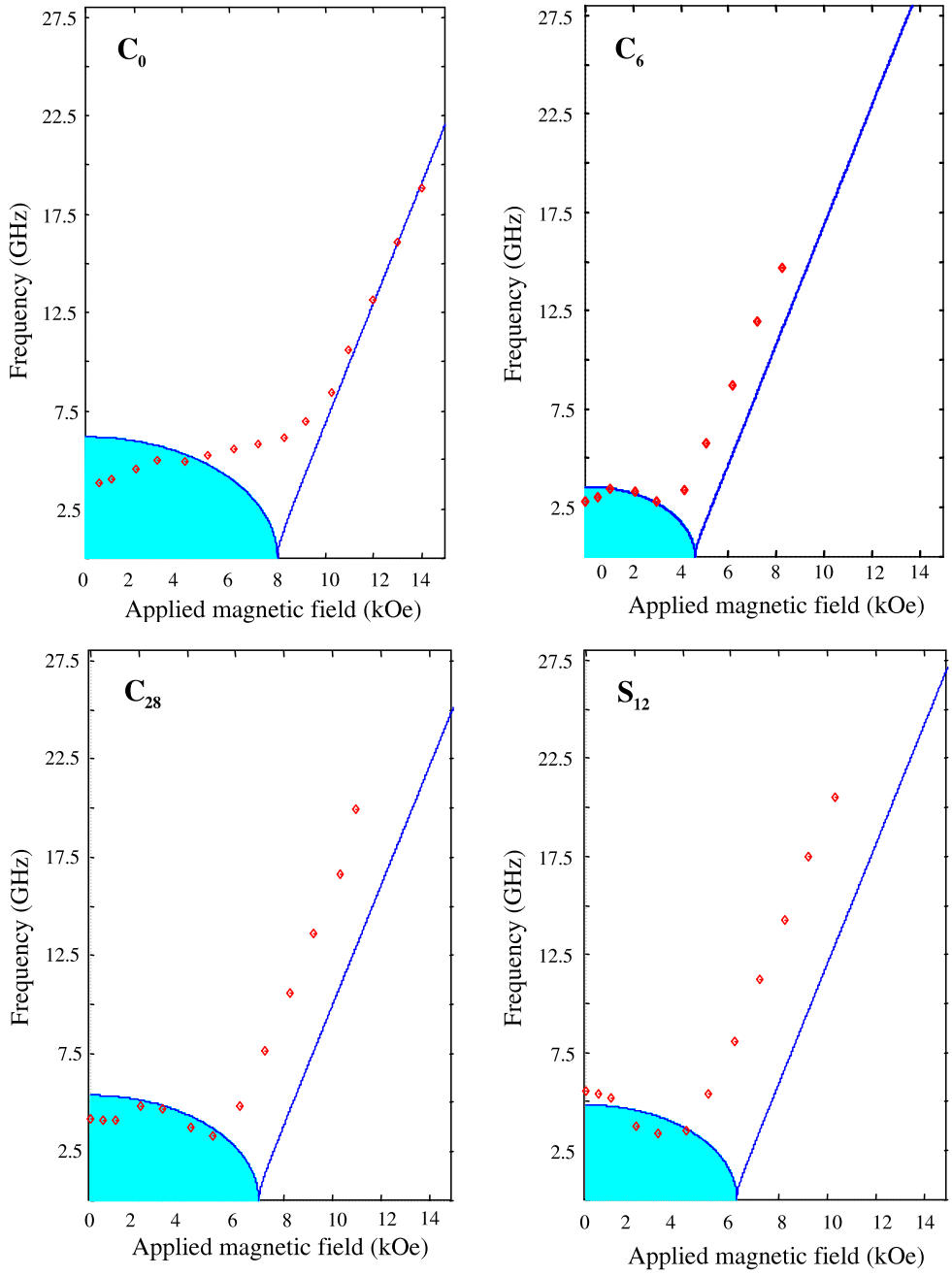

Figure 8. Experimentally observed variations of the frequencies versus the magnetic field applied perpendicularly to the films (with $Q_{\parallel} = 1.43 \times 10^5$ cm^{-1}) compared to the calculated ones, using expression (2) for the energy density.

$[0, (\frac{dQ_{\parallel}}{2})^{0.5}\{4\pi M(4\pi M - H_{a\perp})(1 - (\frac{H}{4\pi M_{eff}})^2)\}^{0.5}]$, will be discussed later.

The experimentally observed variations of the frequency versus H are shown in figure 8. At high magnetic field this variation is linear, as expected. Moreover, in the control sample, the extrapolation of this high field behavior provides a vanishing of the frequency at $H = 4\pi M_{eff} = (4\pi M - H_{a\perp})$. In contrast, surprisingly, for the permalloy films interfaced with NiO, this vanishing does not occur at $H = 4\pi M_{eff}$, but at $H = 4\pi M - (H_{a\perp} + \Delta H_{a\perp})$, where $\Delta H_{a\perp}$, the value of which is reported in table 4, defines a large shift of the anisotropy field. As shown in table 4, the $\Delta H_{a\perp}$ values derived from Brillouin scattering are in satisfactory agreement with the measured ones through the VSM technique. The FMR measurements also provide similar determinations [14].

4.2.2. Oblique applied field. At zero wavevector, for H significantly higher than $4\pi M_{eff}$, expression (2) provides a frequency which depends on the angle α between **H** and the normal to the film and is written as

$$\left(\frac{\omega}{\gamma}\right)^2 = (H - 4\pi M_{eff}(\cos[\alpha])^2)(H - 4\pi M_{eff}((\cos[\alpha])^2 - (\sin[\alpha])^2)). \quad (6)$$

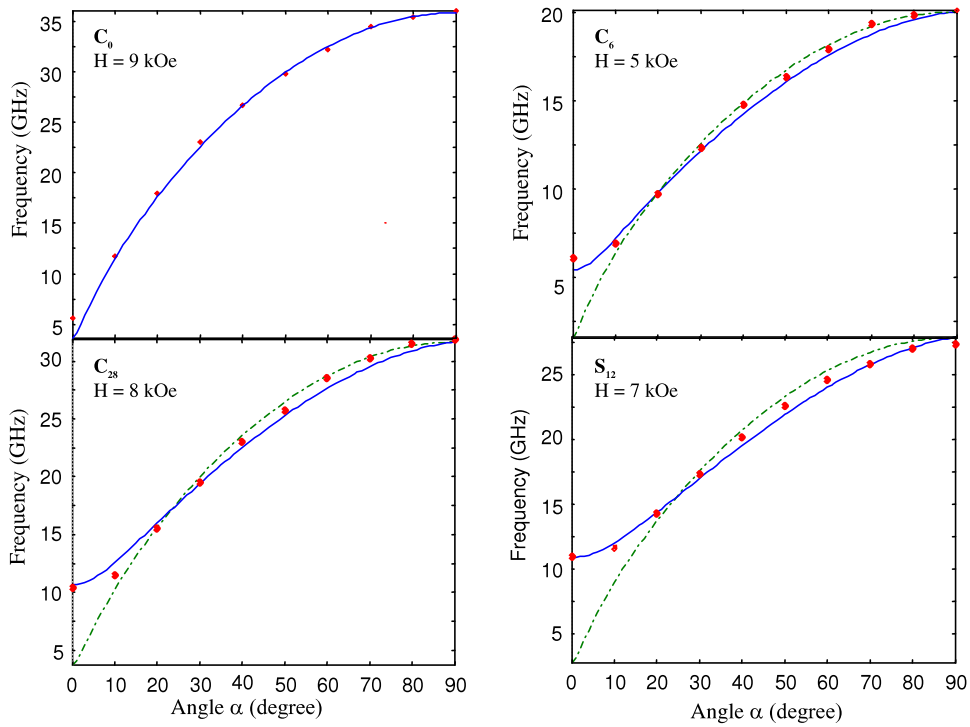

Figure 9. Variation of the Brillouin frequencies versus the angle α between the applied field and the direction normal to the films (with $Q_{\parallel} = 1.43 \times 10^5$ cm^{-1} and $\mathbf{Q}_{\parallel}$ aligned along the in-plane projection of **H**). The full lines represent the best fits using expression (7) for the energy density and the dotted lines are deduced from expression (2).

For the finite $Q_{\parallel}$ values involved in Brillouin scattering, the expected frequency is slightly modified but easily calculated. Experimental variations of the Brillouin frequencies at fixed H versus the angle α are shown in figure 9. For the control sample the results fit well to the calculated ones, using expression (2). In contrast, the presence of NiO gives rise to frequency variations which do not agree with this model. A phenomenological model allows us to restore the fit with experimental data: it consists in introducing an additional term to equation (2) for expressing the energy density, which thus becomes

$$E_f = E - \cos[\alpha]\frac{\Delta K}{M^2}(\mathbf{M}\cdot\mathbf{z})^2 = E - \cos[\alpha]\frac{\Delta H_{a\perp}}{2M}(\mathbf{M}\cdot\mathbf{z})^2 \quad (7)$$

Notice that this additional term does not modify the properties for an in-plane applied field and that it reproduces the results mentioned above for a field perpendicular to the film ($H_{a\perp} \Rightarrow H_{a\perp} + \Delta H_{a\perp}$). As shown in figure 9, this model allows us to fit experimental data, while, for small α values, expression (6) does not provide the observed frequencies. In figure 10, we show the observed frequency dependences versus H for various angles α in two different samples: the agreement with the above described model is satisfactory using expression (7) and would not be using expression (6).

Finally, it is interesting to comment on the obtained spectra for fields perpendicular to the films showing smaller values than in the linear region discussed on in the preceding subsection. The frequency variations versus H are shown in figure 8: they are far from obeying the calculated softening expected at $H = 4\pi M - (H_{a\perp} + \Delta H_{a\perp})$. To interpret this behavior it is important to be aware that, experimentally, it is not possible to insure exact perpendicularity of **H** and that the variation of the frequency versus H deeply depends on the precise value of the misalignment. It results that the softening is dramatically damped by a very small deviation to perpendicularity. It is easy to fit the observed spectra by choosing an adapted misalignment compatible with the experimental uncertainty, as shown in figure 11. In fact, in the vicinity of the perpendicular orientation, many perturbations to the above described model (additional terms, heterogeneity, ...) induce large changes of the frequency variation versus H below the saturation field. Such effects, which are not necessary related to the presence of NiO, can be observed even at zero wavevector, as shown in figure 11 which also reports the variation versus H that we measured by FMR on the control sample using the strip-line technique compared to the Brillouin frequency it is always higher, due, in this last case, to the wavevector dependent contribution.

5. Conclusion

Using different techniques, we have evaluated the magnetic characteristics of permalloy ferromagnetic films interfaced with NiO antiferromagnetic layers. As usual [10, 21], but, up to now, with poor justification, the obtained values derived from high frequency measurements (Brillouin scattering, FMR data) significantly differ from the results of classical magnetometry. We have shown that, contrary to the most common assumption, the exchange bias field direction is not simply related to the direction of the cooling field. In our opinion our

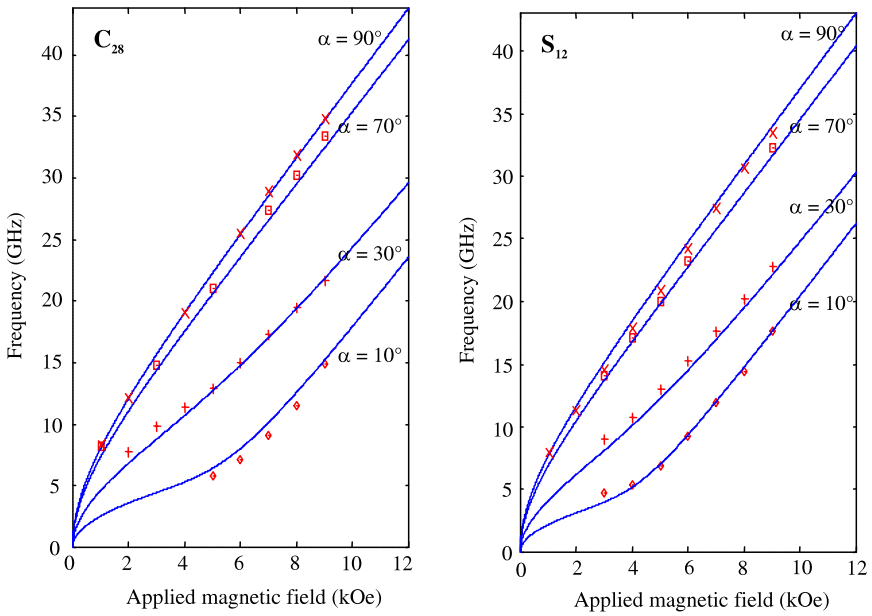

Figure 10. Frequency variations versus the applied magnetic field for various angles α in two different samples. $\mathbf{Q}_\parallel$ ($Q_\parallel = 1.43 \times 10^5$ cm^{-1}) is aligned along the in-plane projection of **H**. For the fitting parameters (full lines), see tables 3 and 4.

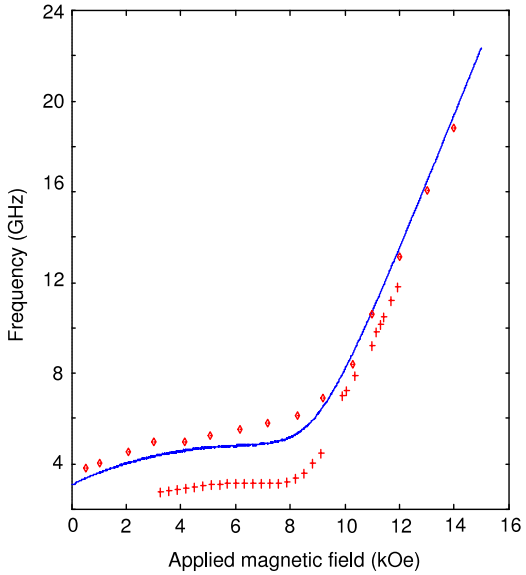

Figure 11. Points: experimentally observed variation of Brillouin frequency versus the magnetic field applied perpendicularly to the film (with $Q_\parallel = 1.43 \times 10^5$ cm^{-1}) in the control sample C_0. Crosses: experimental results of the FMR frequency (using MS-FMR) versus the field applied perpendicularly to sample C_0. The Brillouin frequencies are slightly higher than the FMR ones, due to the non-zero wavevector contribution. Full line: calculated Brillouin frequency in the C_0 sample, using expression (2) for the energy density with $\psi = 60°$ and $\alpha = 3°$ (see the text). Parameters used: $4\pi M_{\text{eff}} = 8000$ G, $\gamma = 1.846 \times 10^7$ Hz G^{-1}, $A = 1 \times 10^{-6}$ erg cm^{-1}.

major contribution is the experimental demonstration that the generally adopted form of the energy density has to be modified in order to account for the frequency variations of the magnetic excitations versus the direction of an out-of-plane applied field. We succeeded in fitting the spectra with the help of the phenomenological introduction of a perpendicular anisotropy field depending upon the direction of the applied field. Such a term presents analogies with the well-known in-plane rotatable field. It is presumably related to some type of interfacial exchange between the antiferromagnetic and the ferromagnetic structures. The investigation of its microscopic origin is in progress.

Acknowledgments

We acknowledge Dr H Hurdequint from the Laboratoire de Physique des Solides (CNRS, Université Paris 11, France) who prepared the samples and kindly communicated to us his own data concerning FMR results, and we also acknowledge Dr K Bouziane from the College of Science (Sultan Qaboos University, Oman) for the VSM measurements.

References

[1] Meiklejohn W H and Bean C P 1956 *Phys. Rev.* **102** 1413
[2] Nogués J and Schuller I K 1999 *J. Magn. Magn. Mater.* **192** 203
[3] Stamps R L 2000 *J. Phys. D: Appl. Phys.* **33** R247
[4] Nogués J, Sort J, Langlais V, Skumryev V, Suriñach S, Muñoz J S and Baro M D 2005 *Phys. Rep.* **422** 65
[5] Kiwi M 2001 *J. Magn. Magn. Mater.* **234** 584
[6] McMichael R D, Stiles M D, Chen P J and Egelhoff W F 1998 *Phys. Rev.* B **58** 8605
[7] Wee L, Stamps R L, Malkinski L and Celinski Z 2004 *Phys. Rev.* B **69** 134426
[8] Geshev J, Pereira L G and Schmidt J E 2002 *Phys. Rev.* B **66** 134432
[9] Saito N, Fujiwara H and Sugita Y 1964 *J. Phys. Soc. Japan* **19** 421
[10] Miltényi P, Gruyters M, Güntherodt G, Nogués J and Schuller I K 1999 *Phys. Rev.* B **59** 3333

[11] Rezende S M, Lucena M A, Azevedo A, de Aguiar F M, Fermin J R and Parkin S S P 2003 *J. Appl. Phys.* **93** 7714
[12] Gogol P 2000 *Ph.D. Thesis* Université Paris Sud
[13] Hurdequint H 2002 *J. Magn. Magn. Mater.* **521** 242
[14] Hurdequint H 2004 *IWEBMN2004 (Anglet, Sep)* pp 85–6 (Abstract)
[15] Moch P, Djémia P and Ganot F 2001 *Le Vide* **56** 565–80
[16] Meiklejohn W P 1962 *J. Appl. Phys.* **33** 1328
[17] Labrune M, Kools J C S and Thiaville A 1997 *J. Magn. Magn. Mater.* **171** 1
[18] Zighem F, Roussigné Y, Chérif S-M and Moch P 2007 *J. Phys.: Condens. Matter* **19** 176220
[19] Stamps R L 1994 *Phys. Rev.* B **49** 339
[20] Rezende S M, Azevedo A, Lucena M A and de Aguiar F M 2001 *Phys. Rev.* B **63** 214418
[21] Fermin J R, Azevedo M A, de Aguiar F M and Rezende S M 2000 *J. Appl. Phys.* **87** 6421
[22] Zighem F, Ben-Youssef J, Roussigné Y, Chérif S-M and Moch P 2008 at press